Volume 5, Issue 7, pp. 58-73, 2021.
International Journal of Scientific Engineering and Science
ISSN (Online): 2456-7361

Experimental and Micro-Macro Mechanics Methods in Prediction of Mechanical Properties of Carbon Fibre-Reinforced Composite Panels

Umar Farooq[*1], Peter Myler[2], Mahmoona Siddique[3]
[1, 2]Faculty of Engineering, Support and Advanced Sciences, University of Bolton BL3 5AB, United Kingdom
Email: U.Farooq @ bolton.ac.uk, pm8 @ bolton.ac.uk
[3]Lecturer, Department of Mathematics, Government Degree College for Women, Sargodha 4000 Pakistan. Email: monamaths0 @ gmail.com

Abstract— *This paper is concerned with predictions of mechanical properties of carbon fibre-reinforced laminated composite panels using micro-macro mechanics laws. Due to superior mechanical properties, the fibrous composites are being increasingly used in aircraft industry. The industry attaches prime importance to experimental testing methods to screen quality mechanical properties of fibrous composite made components at pre-design level. However, different test methods and setups produce different results, while analytical studies neglect influence from coupling deformations. That necessitates use of micro-macro mechanics methods to be included to supplement the existing methods. Present work is mainly based on usage of micro-macro mechanics laws and influence from deformations to enhance previous efforts in prediction of mechanical properties. Current study progresses with determining properties from physical tests and relating them to off-axes properties to develop two- and three-dimensional mathematical formulations. Computer programs for the formulations were written and implemented in MATLAB[TM] software to predict the properties. Good agreement was found between predicted and experimental produced quantities of the mechanical properties. Comparisons of results confirmed that proposed use of micro-macro mechanics laws could efficiently predict mechanical properties the panels considered in current study.*

Keywords— *A. Polymer Matrix Composites; B. Mechanical Property; C. Material Testing Methods.*

I. INTRODUCTION

Fiber-reinforced composite panels are manufactured from combination of fibres and resin rich matrices. The combined constituents keep their individual characteristics while creating a new substance of superior properties in a specific application [1]. Fibers are deliberately oriented in matrices to increase directional stiffness of the materials. Plies are stacked in various orientations of fibre directions to build composite panels [2]. The most efficient configuration to effectively transfer forces for a unidirectional force system is a unidirectional composite panel oriented in the direction of loading path [3]. In cases where loading are such that unidirectional panels are inadequate or inefficient then multi-directional panels are used. The composites are being used as alternatives to steel due to their outstanding corrosion resistance, high specific strength properties (20-40% weight savings), low cost, long service life, and reduced maintenance. The other common desirables consist of the following: ability to fabricate directional mechanical properties, excellent fatigue and fracture resistance, lower tooling cost alternatives, lower thermal expansion properties, simplification of manufacturing by parts integration, potential for rapid process cycles, and ability to meet stringent dimensional stability requirements. Because of favourable properties, the composite materials are being widely used in modern aircraft structures as shown in Figure 1 [4], and their applications are rapidly expanding in military vehicles, ships, buildings, and offshore structures.

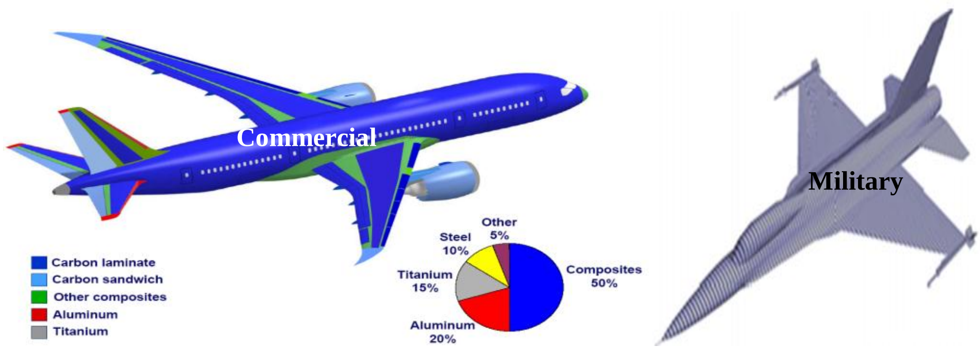

a) b)
Figure 1: Images of a) commercial, b) military aircrafts

Since composite panels possess anisotropic properties whereby a normal stress may induce both normal and shear strains hence relationships between forces and deformations exhibit much more complication compared to conventional materials [5].

International Journal of Scientific Engineering and Science
Volume 5, Issue 7, pp. 58-73, 2021. ISSN (Online): 2456-7361

These coupling effects have important implications in mechanics of composites and characterization of mechanical properties to understand their unexpected behaviour structural components during service life [6]. Thus extensive research work is being carried out on various aspects of mechanical properties characterizations of the composites. Selected ones are being presented below for reference.

Structural elements have certain characteristics of shape, rigidity, stiffness, and strength [7]. Thus comprehensive knowledge of their characteristic properties is important before using them as load bearing components. Various physical testing methods are used for screening properties of materials before they are used put into work. Basic **'**ignition loss method' is used to determine quantities of volume fractions by weight in a composite panel. The characteristic properties identify parameters that influence strengths and response of composite materials such as fibre, matrix types and interfaces [8]. These volume fractions quantities are utilised in Rule of Mixture (ROM), Halping-Tsai relations, and physical testing to formulate relationships among basic mechanical properties so that the property data can further be used to evaluate performance of the composite panels [9]. Common experimental methods to predict properties of composite materials consist of the tensile, compression, flexural, shear modulus, Iosipescu, and v-notch-rail detailed in [10]**.** Young's modulus is one of the important characteristic; however, factors affecting its determination are complicated: nature of matrix and filler, compatibility, and material processing technology [11] and [12]. Similarly, dispersion or distribution of the filler in the matrix, interfacial structure and morphology affect the modulus [13] and [14]. Influence of shear effects in the displacements is another important factor, larger span-to-depth ratios are used to reduce the influence [14]. It is reported in [16] that fibre reinforced composites are inhomogeneous and anisotropic in nature hence their characterisation is complex. Laminates with aligned reinforcement are stiff along the fibres, but weak in transverse to the fibre direction [17]. In order to obtain equal stiffness in all off-axis loading systems to present balanced angle plies were investigated in [18] and [19]. To obtain equal stiffness in all directions quasi-isotropic lay-up configurations were used in [20] and [21]. These methods relate material properties into algebraic set of equations that are easier to code and solve using computers [31], [23]. However, use of the method is reported to be limited for cases of tensile-shear interaction if the off-axis loading system does not coincide with the main axes of a single lamina or if the panel is not balanced. Instead of such testing, the simplified property prediction schemes based on mathematical formulations were preferred in [24] and [25]. A composite laminate subjected to off-axis loading system presents tensile-shear interactions in its plies that leads to distortions and local micro-structural damage hence their testing can produce unreliable results. Thus, unidirectional lamina was tested at different fibre volume fractions to predict elastic constants using the finite element method [26] and [27]. The study paved the way for solution to obtain equal stiffness of panels subjected in all directions within a plane is presented by various authors by stacking and bonding together plies with different fibres orientations. Allocations of appropriate input engineering parameters such as the effective elastic moduli and the associated Poisson's ratios for materials based on the theory of micro-macro mechanics along with linear elasticity and their limitations are detailed in [28], [29], and [30]. Characterization of in-plane mechanical properties of laminated hybrid composites is given in [31], and mechanics-of-materials model for predicting Young's modulus of damaged woven fabric composites, involving three damage modes can be found in [32].

The literature review reveals that majority of the existing studies are experimental, resource and time consuming. Many test methods use different geometries for panels and holding-fixtures that produce different data. Researcher has to undergo series of experiments to obtain desired properties [33]. Moreover, composites are anisotropic in nature while certain characteristics of shape, rigidity, and strength make physical testing complicated [34]. Furthermore, analytical studies based on neglecting deformation effects could not be relied to predict optimal mechanical properties [35]. Micro-macro mechanics based theoretical methods are required to evaluate performance and identify load bearing parameters panels.

Current study is mainly based on micro-macro mechanics of fibrous composites. Stiffness matrices and invariants were formulated to include stress-strain effects and implemented in MATLAB^{TM} code to approximate the properties. Comparison and validation were carried out against intra-simulation and experimentally produced results and found within acceptable agreement. The study proposed that mechanical properties can be reliably determined from computer codes utilising the micro-macro mechanics laws.

II. MATERIALS AND METHODS

2.1 Carbon fibre-reinforced panel and material properties

General realisation is that a comprehensive analysis programme to investigate the mechanical properties of a full-scale structure would prove too costly. Thus, smaller representative specimens are normally studied using restricted parameters under specific conditions so that the scale effect is accounted for, and data could be used at pre-design evaluation of full-scale structures. Moreover, composites are heterogeneous materials hence full characterisation of their properties is difficult, as various processing factors may influence the properties: misaligned fibres, fibre damage, non-uniform curing, cracks, voids and residual stresses. These factors are assumed to be negligible when care is taken in the manufacturing processes. Considering these reasons, the purpose specific fabricated panels supplied by manufacturer were considered. Brief illustrations of carbon fibres, satin weave 5th ply harness layup, and schematic of 8-, 16-, and 24-Ply beam-panels with plane dimensions: 150mm x 120mm are shown in [2].

International Journal of Scientific Engineering and Science
Volume 5, Issue 7, pp. 58-73, 2021. ISSN (Online): 2456-7361

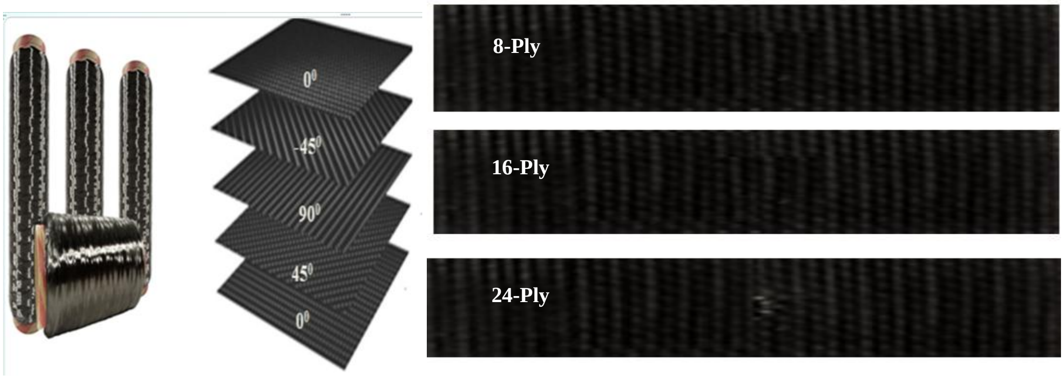

Figure 2: Schematic a) fibres, b) 5th harness satin weave, and c) beam specimens

Panels considered were of code Fibredux 914C-833-40, consisting of 8-, 16-, and 24-Ply layup, assumed to be void-free, Poison's ratio: 0.21, and property parameters given in Table 1.

Table 1: Panels, layup codes, average thickness, and properties

Panel	Lay-up code	Thickness mm	Property parameter	Unit MPa
8-Ply	$[0/90/45/-45]_S$	2.4	E_{xx} (0^0), E_{yy} (90^0)	230
16-Ply	$[0/90/45/-45]2_S$	4.8	τ_{xy} 45^0, -45^0	23
24-Ply	$[0/90/45/-45]3_S$	7.2	Gxy	88

2.2 Experimental test methods

An important aspect of the subject is the physical testing of material samples by applying forces and deformations. Once behaviour of material is quantitatively known from testing, its chances of success in a particular engineering design could be evaluated. When a material is characterised experimentally, its mechanical properties (engineering constants) are measured instead of the stiffness or the compliance. This is because mechanical properties can be easily defined and interpreted in terms of simple state of stress and strain used in design development and analysis. Mechanical properties of the test standard panels are obtained from static experimental test methods: tensile, compression, flexural, shear modulus as shown in Figure 3, for details please refer to (ASTM: D7264). Tensile and bending tests suffice requirements of current study; therefore, compression and shear testing procedures and discussion of their results will not be included.

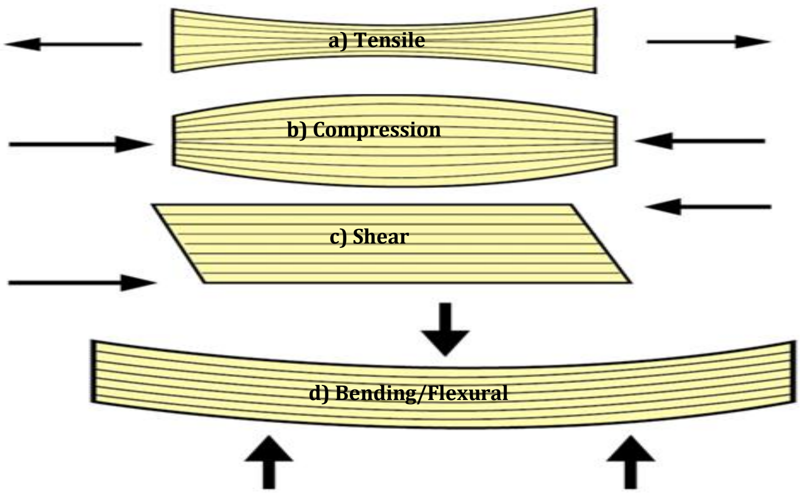

Figure 3: Schematics of common test methods for composite panels

Commonly used universal machine for the above tension, compression, flexure tests is shown in Figure 4 below.

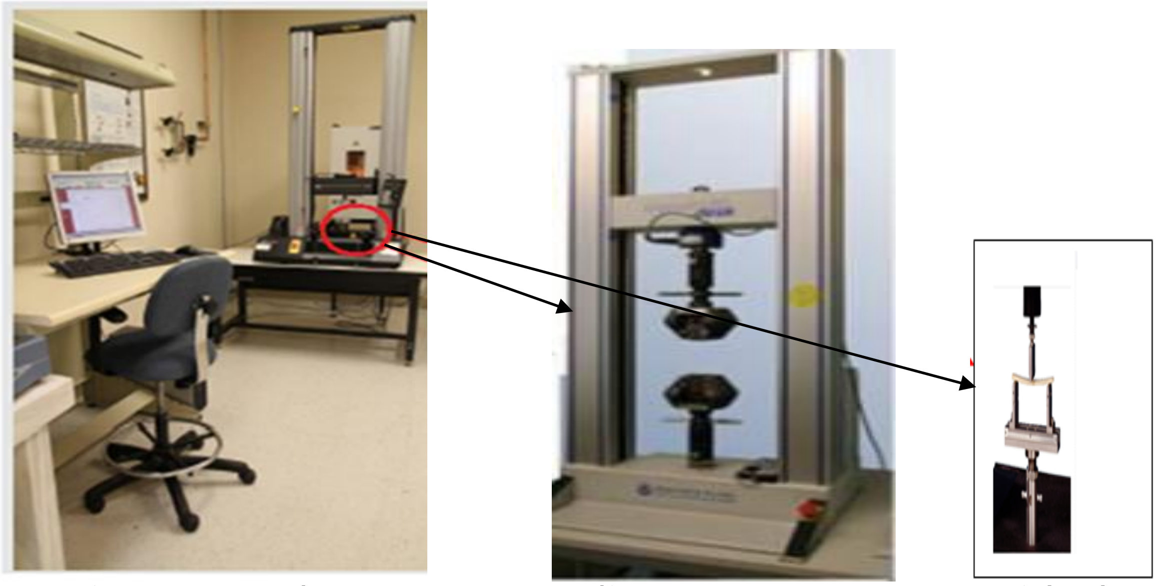

a) InstranTM 5585H machine b) Tension/compression c) Flexural

Figure 4: Images of a) Machine, b), and c) enlarged view of chambers

2.2.1 Tensile test

Three specimens from each of the panels were prepared in I-shapes in line with the testing standard for tensile tests (ASTM: D3039). Photographs of the specimens selected for the tests are shown in Figure 2(c). Average span and width of 8-, 16-, and 24-Ply specimens were considered 120mm and 20mm with average thicknesses considered 2.4, 4.8, and 7.2mm, respectively. The effective beam length (L) used for all calculations was length (120mm) –both the grips (30mm) = 90mm, approximate dimensions and relevant spans to depth ratios as shown in Figure 5. Load transfer tabs were adhesively bonded to the ends of the specimens in order that the load may be transferred from the grips of the tensile testing machine to the specimen without damaging it. Specimens were gripped at both ends. The specimen was inserted within in the fixture holders of the machine by metal grips as shown in and loaded axially at a rate of 1 mm/min. The applied tensile load produced tensile stresses through the holding grips that results elongation of the specimen in loading direction.

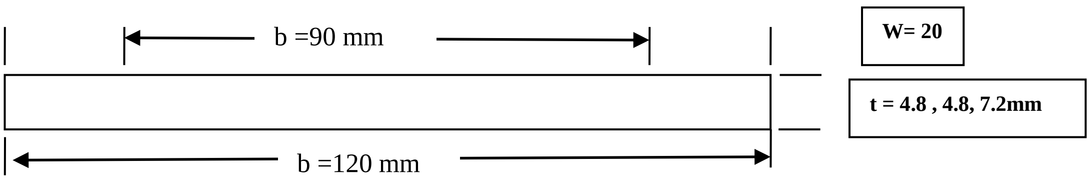

a) b)

Figure 5: Schematic of a) beam panel, b) cross-sectional area

Results from two beam specimens were selected from the three types of panels shown in Figure 2(c). Approximate mechanical properties predicted by tensile experimental tests are presented in Table 3.

2.2.2 Flexural test

Flexural properties of the specimens were determined using the standard method of three point bending test. A schematic of simply supported flat rectangular specimens three types closed at both ends with cross-sectional areas of constant width is shown in Figure 6. The specimens have different thicknesses: t= 2.4, 4.8, 7.2mm, as can be seen from Figure 5. There is a wide variety of test methods available for flexure testing described in (ASTM: D7264) those address particular testing needs of heterogeneous, non-isotropic materials.

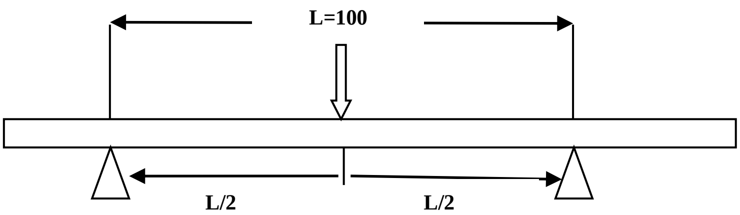

Figure 6: Schematics of specimen under three-point bending

The vertically applied load could deflect (bend) the specimen and could even fracture the outer fibres under excessive loading. Approximate dimensions and relevant simple support of span to depth ratios provides base to be utilised in beam bending formulation. Calculation of Young's modulus from the load-displacement relations are given in
Table 2.

Table 2: Formulation used to calculate young's modulus.

Bending moment	Area moment	Max Bending Stress	Load	Young's modulus
$M = P\frac{L}{4}$	$I = \frac{wt^3}{12}$	$\sigma_{max} = \frac{M\left(\frac{t}{2}\right)}{I} = \frac{3}{2}\frac{PL}{wt^2}$	$P = \frac{3}{2}\frac{\sigma wt^2}{L}$	$E = \frac{PL^3}{48I\delta}$

Approximate mechanical properties for three types of specimens in Figure 2(c) predicted by tensile and three-point bending tests are compared and illustrated in Table 3 below.

Table 3: Young's modulus of beam specimens

Specimen	**Young's modulus GPa**			
	Tensile test		**Flexural Test**	
	1	**2**	**1**	**2**
8-Ply	45.8	45.2	52.8	53.2
16-Ply	45.5	45.7	51.5	49.2
24-Ply	48.4	49.1	48.6	49.8

2.3 Micro-macro mechanics methods to determine engineering properties

2.3.1 Use of Rule of Mixture properties in orthotropic lamina formulations

Most of the structural parts use laminates that consist of several plies with different orientations connected together through a bonding interface. A lamina (heterogeneous at the constituent level) forms the building block of laminated composites based structures. Micromechanics do not refer to mechanical behaviour at the molecular level rather it looks at components of a composite lamina (matrix and fibre) while behaviour of the lamina is called "macro-mechanics" those predict behaviour of the assumed homogeneous composite material. Mechanical and physical properties of the lamiae (reinforcement and matrix) and their interactions are examined on a micro-macroscopic level on various degrees of simplifications. Fibre and matrix densities are measured and converted into respective fibre volume fractions that form basis for approximation of engineering properties [14]. Elastic constants (for uniformity expressed in normal format rather than italic) for unidirectional lamina with fibres aligned in x direction can be calculated using Rule of Mixture from the following equations:

$\mathrm{E_L} = \mathrm{E_f V_f} + \mathrm{E_m V_m}$ (Longitudinal Young's modulus) **(1)**

$\mathrm{E_T} = \frac{\mathrm{E_f E_m}}{\mathrm{E_f V_m} + \mathrm{E_m V_f}}$ (Transverse Young's modulus) **(2)**

$\mathrm{G_{LT}} = \frac{\mathrm{E_L}}{2(1+\nu_{\mathrm{LT}})}$ (In-plane shear modulus) **(3)**

$\nu_{\mathrm{LT}}\mathrm{E_T} = \nu_{\mathrm{TL}}\mathrm{E_L}$ (Relation for Poisson's ratios) **(4)**

Equations (1)-(4) can be utilised to determine components of the lamina stiffness matrix (Q), and subscripts L and T are replaced by 1 & 2:

$$Q_{11} = \frac{E_1}{1-\upsilon_{12}\upsilon_{21}}, Q_{12} = \frac{\upsilon_{12}E_2}{1-\upsilon_{12}\upsilon_{21}} = Q_{21}, Q_{22} = \frac{E_2}{1-\upsilon_{12}\upsilon_{21}}, \text{and } Q_{66} = G_{12},$$

Elastic constants are required to consider influence from in-plane deformations. Out-of-plane stresses ($\sigma_{zz} = \tau_{xz} = \tau_{yz} = 0$) may be neglected for the stress-strain relations of a thin elastic lamina.

$$\varepsilon_{xx} = \frac{1}{E}\left(\sigma_{xx} - \upsilon\sigma_{yy}\right)$$
$$\varepsilon_{yy} = \frac{1}{E}\left(-\upsilon\sigma_{xx} + \sigma_{yy}\right)$$
$$\gamma_{xy} = \frac{1}{G}\left(\tau_{xy}\right) \quad \textbf{(5)}$$

There is no coupling between the shear stresses and normal stress. For an orthotropic lamina in a plane stress form as shown in Figure 7, the stress-strain relations may be written:

$$\varepsilon_{xx} = \frac{\sigma_{xx}}{E_{xx}} - \upsilon_{yx}\frac{\sigma_{yy}}{E_{yy}} - m_x\tau_{xy}$$
$$\varepsilon_{yy} = -\upsilon_{xy}\frac{\sigma_{xx}}{E_{xx}} + \frac{\sigma_{yy}}{E_{yy}} - m_y\tau_{xy}$$
$$\gamma_{xy} = -m_x\sigma_{xx} - m_y\sigma_{yy} + \frac{\tau_{xy}}{G_{xy}} \quad \textbf{(6)}$$

International Journal of Scientific Engineering and Science
Volume 5, Issue 7, pp. 58-73, 2021.
ISSN (Online): 2456-7361

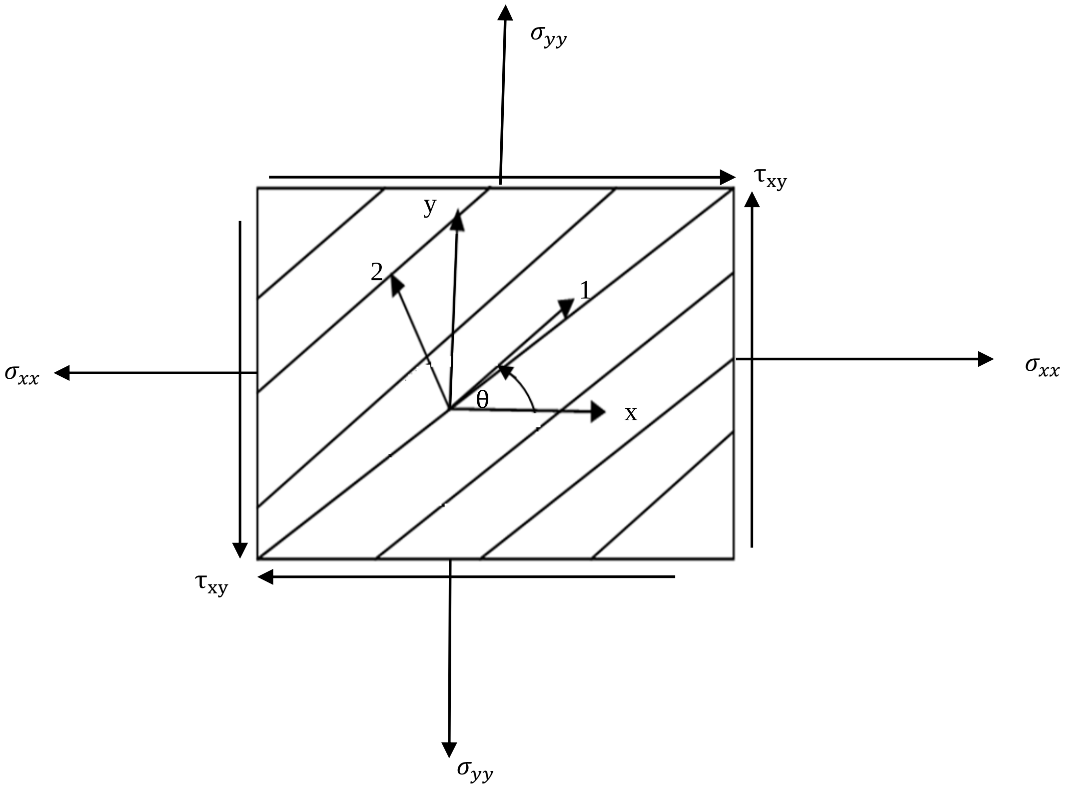

Figure 7: Orthotropic lamina in a plane stress

Stresses in a general orthotropic lamina under a plane stress conditions may be obtained from coefficients of mutual influence (m_x and m_y) for an angle-lamina in global coordinates can be determined from the equations:

$$m_x = (\sin 2\theta)\left[\frac{\nu_{12}}{E_{11}} + \frac{1}{E_{22}} - \frac{1}{2G_{12}} - (cos^2\theta)\left(\frac{1}{E_{11}} + \frac{2\nu_{12}}{E_{11}} + \frac{1}{E_{22}} - \frac{1}{G_{12}}\right)\right] \quad \textbf{(7)}$$

$$m_y = (\sin 2\theta)\left[\frac{\nu_{12}}{E_{11}} + \frac{1}{E_{22}} - \frac{1}{2G_{12}} - (sin^2\theta)\left(\frac{1}{E_{11}} + \frac{2\nu_{12}}{E_{11}} + \frac{1}{E_{22}} - \frac{1}{G_{12}}\right)\right] \quad \textbf{(8)}$$

For an especially orthotropic lamina ($\theta = 0^0$ and 90^0), the stress-strain relations yield:

$$\varepsilon_{xx} = \varepsilon_{11} = \frac{\sigma_{xx}}{E_{11}} - \upsilon_{21}\frac{\sigma_{yy}}{E_{22}}$$

$$\varepsilon_{yy} = \varepsilon_{22} = -\upsilon_{12}\frac{\sigma_{xx}}{E_{11}} + \frac{\sigma_{yy}}{E_{22}}$$

$$\gamma_{xy} = \gamma_{yx} = \gamma_{12} = \gamma_{21}\frac{\tau_{xy}}{G_{xy}} \quad \textbf{(9)}$$

The relations may be written in local coordinates as

$$\begin{Bmatrix}\sigma_1\\ \sigma_2\\ \tau_{12}\end{Bmatrix} = \begin{bmatrix}Q_{11} & Q_{12} & 0\\ Q_{12} & Q_{22} & 0\\ 0 & 0 & Q_{66}\end{bmatrix}\begin{Bmatrix}\varepsilon_1\\ \varepsilon_2\\ \frac{\gamma_{12}}{2}\end{Bmatrix} \quad \textbf{(10)}$$

Similarly, for the general orthotropic lamina ($\theta \neq 0$ and 90), the complete set of transformation equations for the stresses in the xy-coordinate system can be developed using the local-global coordinate transformation matrix

$$\begin{Bmatrix}\sigma_1\\ \sigma_2\\ \tau_{12}\end{Bmatrix} = [T]\begin{Bmatrix}\sigma_x\\ \sigma_y\\ \tau_{xy}\end{Bmatrix} \quad \textbf{(11)}$$

Where: $[T] = \begin{bmatrix}m^2 & n^2 & 2mn\\ n^2 & m^2 & -2mn\\ -mn & mn & m^2 - n^2\end{bmatrix}; m = \cos\theta \; and \; n = \sin\theta$

The generally orthotropic laminate creates fully populated, the reduced transformed stiffness matrix:

$$\begin{Bmatrix}\sigma_x\\ \sigma_y\\ \tau_{xy}\end{Bmatrix} = \begin{bmatrix}\bar{Q}_{11} & \bar{Q}_{12} & \bar{Q}_{16}\\ \bar{Q}_{12} & \bar{Q}_{22} & \bar{Q}_{26}\\ \bar{Q}_{16} & \bar{Q}_{26} & \bar{Q}_{66}\end{bmatrix}\begin{Bmatrix}\varepsilon_x\\ \varepsilon_y\\ \gamma_{xy}\end{Bmatrix} \quad \textbf{(12)}$$

Where: $\bar{Q}_{ij}$ are the components of the transformed stiffness matrix defined as follows:

$$\bar{Q}_{11} = Q_{11}cos^4\theta + Q_{22}sin^4\theta + 2(Q_{12} + 2Q_{66})sin^2\theta cos^2\theta$$

$\bar{Q}_{12} = (Q_{11} + Q_{22} - 4Q_{66})sin^2\theta cos^2\theta + Q_{12}(cos^4\theta + sin^4\theta)$
$\bar{Q}_{22} = Q_{11}cos^4\theta + Q_{22}sin^4\theta + 2(Q_{12} + 2Q_{66})sin^2\theta cos^2\theta$
$\bar{Q}_{16} = (Q_{11} - Q_{12} - 2Q_{66}) \sin\theta\, cos^3\theta - (Q_{22} - Q_{12} - 2Q_{66}) \cos\theta\, sin^3\theta$
$\bar{Q}_{26} = (Q_{11} - Q_{12} - 2Q_{66}) \cos\theta\, sin^3\theta - (Q_{22} - Q_{12} - 2Q_{66}) \sin\theta\, cos^3\theta$
$\bar{Q}_{66} = (Q_{11} + Q_{22} - 2Q_{12} - 2Q_{66})sin^2\theta cos^2\theta + Q_{66}(cos^4\theta + sin^4\theta)$

It appears from Eq. (12) that there are six constants that govern the stress-strain behaviour of a lamina. However, the equations are linear combinations of the four basic elastic constants, and therefore are not independent. Elements in stiffness matrices can be expresses in terms of five invariant properties of the lamina using trigonometric identities:

$\bar{Q}_{11} = U_1 + U_2cos2\theta + U_3cos4\theta$
$\bar{Q}_{12} = U_4 - U_3cos4\theta$
$\bar{Q}_{22} = U_1 - U_2cos2\theta + U_3cos4\theta$
$\bar{Q}_{16} = \frac{U_2}{2}sin2\theta + U_3sin4\theta$
$\bar{Q}_{26} = \frac{U_2}{2}sin2\theta - U_3sin4\theta$
$\bar{Q}_{66} = \frac{1}{2}(U_1 - U_4) - U_3 \cos 4\theta$ **(13)**

Where the set of invariants is defined as

$U_1 = \frac{1}{8}(3Q_{11} + 3Q_{22} + 2Q_{12} + 4Q_{66})$
$U_2 = \frac{1}{2}(Q_{11} - Q_{22})$
$U_3 = \frac{1}{8}(Q_{11} + Q_{22} - 2Q_{12} - 4Q_{66})$
$U_4 = \frac{1}{8}(3Q_{11} + 3Q_{22} + 6Q_{12} - 4Q_{66})$ **(14)**

The invariants due to rotations in Eq. (14) are simply linear combinations in plane of the lamina. There are four independent invariants, just as there are four independent elastic constants. In the equation, all the stiffness expressions (except coupling) consist of one constant term which varies with lamina orientations. Thus, the effects of lamina orientation on stiffness are easier to interpret very useful in computing elements of these matrices. The element of fibre-reinforced composite material with its fibre oriented at some arbitrary angle exhibits a shear strain when subjected to a normal stress, and it also exhibits an extensional strain when subjected to a shear stress. The state of stress is defined as $\sigma_{xx} \neq 0, \sigma_{yy} = \tau_{xy} = 0$.

Mutual influence coefficients can be found from:

$\eta_{x,xy} = \frac{\gamma_{xy}}{\varepsilon_{xx}}$ **(15)**

Similarly, when the state of stress is defined as $\sigma_{yy} \neq 0, \sigma_{xx} = \tau_{xy} = 0$, the ratio

$\eta_{y,xy} = \frac{\gamma_{xy}}{\varepsilon_{yy}}$ **(16)**

As pure shear stresses $\tau_{xy} \neq 0, \sigma_{xx} = \sigma_{yy} = 0$, the ratio $\eta_{xy,y}$ characterises the normal strain response along the y direction due to a shear stress in the x-y plane. The ratio can be found as:

$\eta_{xy,y} = \frac{\tau_{xy}}{G_{xy}}$ **(17)**

Superposition of loading, stress-strain relations in terms of elastic constants are:

$$\begin{Bmatrix}\varepsilon_{xx}\\ \varepsilon_{yy}\\ \gamma_s\end{Bmatrix} = \begin{bmatrix}\frac{1}{E_{xx}} & -\frac{\nu_{yx}}{E_{yy}} & \frac{\eta_{sx}}{G_{xy}}\\ -\frac{\nu_{yx}}{E_{xx}} & \frac{1}{E_{yy}} & \frac{\eta_{sy}}{G_{xy}}\\ \frac{\eta_{sx}}{G_{xy}} & \frac{\eta_{sy}}{G_{xy}} & \frac{1}{G_{xy}}\end{bmatrix}\begin{Bmatrix}\sigma_{xx}\\ \sigma_{yy}\\ \tau_s\end{Bmatrix} \quad \textbf{(18)}$$

Elastic constants derived from Eq. (18) in global coordinates can be written as:

$$E_{xx} = 1 \Big/ \left[\frac{m^2}{E_{11}}(m^2 - n^2\nu_{12}) + \frac{n^2}{E_{22}}(n^2 - m^2\nu_{12}) + \frac{m^2n^2}{G_{12}}\right] \quad \textbf{(19)}$$

$$E_{yy} = 1 \Big/ \left[\frac{n^2}{E_{11}}(n^2 - m^2\nu_{12}) + \frac{m^2}{E_{22}}(m^2 - n^2\nu_{21}) + \frac{m^2n^2}{G_{12}}\right] \quad \textbf{(20)}$$

$$G_{xy} = 1 \Big/ \left[\frac{4m^2n^2}{E_{11}}(1 + \nu_{12}) + \frac{4m^2n^2}{E_{22}}(1 + \nu_{21}) + \frac{(m^2-n^2)^2}{G_{12}}\right] \quad \textbf{(21)}$$

$$\nu_{xy} = E_{xx} \Big/ \left[\frac{m^2}{E_{11}}(m^2\nu_{12} - n^2) + \frac{n^2}{E_{22}}(n^2\nu_{12} - m^2) + \frac{m^2n^2}{G_{12}}\right] \quad \textbf{(22)}$$

Volume 5, Issue 7, pp. 58-73, 2021. ISSN (Online): 2456-7361

$$\nu_{yx} = {E_{yy}\nu_{xy}}/{E_{xx}} \quad \textbf{(23)}$$

$$\eta_{xs}/E_{xx} = \eta_{sx}/G_{xy} = \left[\frac{2m^3n}{E_{11}}(1+\nu_{12}) - \frac{2mn^3}{E_{22}}(1+\nu_{21}) - \frac{mn(m^2-n^2)}{G_{12}}\right] \quad \textbf{(24)}$$

$$\eta_{ys}/E_{yy} = \eta_{sy}/G_{xy} = \left[\frac{2mn^3}{E_{11}}(1+\nu_{12}) - \frac{2nm^3}{E_{22}}(1+\nu_{21}) + \frac{mn(m^2-n^2)}{G_{12}}\right] \quad \textbf{(25)}$$

2.3.2 Effective mechanical properties for three-dimensional panels

Real structural elements involve lay-ups containing various number of angle plies subjected to three-dimensional state of stresses. Engineering properties using 'Rule of Mixture' may be written as:

$$E_x = \frac{1}{3}E_L + \frac{2}{3}E_T \quad \textbf{(26)}$$

$$E_y = \frac{2}{3}E_L + \frac{1}{3}E_T \quad \textbf{(27)}$$

$$E_z = E_T \quad \textbf{(28)}$$

$$\nu_{nm}E_m = \nu_{mn}E_n \quad \textbf{(29)}$$

Shear moduli may be written as follows:

$$G_{xy} = \frac{\tau_{xy}}{\gamma_{xy}},\ G_{xz} = \frac{\tau_{xz}}{\gamma_{xz}},\ G_{yz} = \frac{\tau_{yz}}{\gamma_{yz}}, \quad \textbf{(30)}$$

Where: L stands for longitudinal and T for transverse directions.

The determination of the material properties of laminate with several layers of lamina and orientations can be done using the theory of lamination plates. The deformation hypothesis from classical homogeneous plate theory and the laminated force-deformation equation can be used to define the coordinate system in developing the relations. The force, *N* and moment, *M* per unit length for the laminate, which can be computed at ply level. The quadratic mid-plane of the laminate contains x-y axes, and z axis defines the thickness direction. A typical laminate geometry of thickness h, number of laminas N, and lamina thickness t is shown in sketch Figure 8.

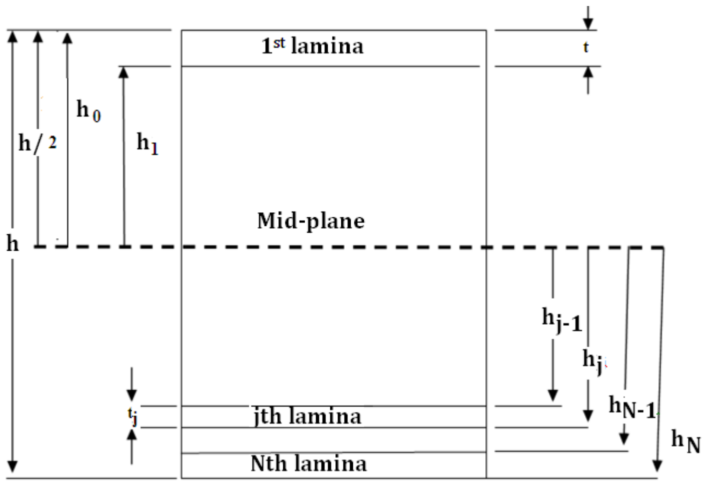

Figure 8: Laminate geometry coordinate locations of ply in a laminate

Laminate strains are linearly related to the distance from the mid-plane:

$$\varepsilon_{xx} = \varepsilon_{xx}^0 + zk_{xx}$$
$$\varepsilon_{yy} = \varepsilon_{yy}^0 + zk_{yy}$$
$$\gamma_{xy} = \gamma_{xy}^0 + 2zk_{xy} \quad \textbf{(31)}$$

Where:

$\varepsilon_{xx}^0, \varepsilon_{yy}^0$ = mid-plane normal strains in the laminate

γ_{xy}^0 = mid-plane shear strain in the laminate

$k_{xx}\ k_{yy}$ = bending curvatures in the laminate

k_{xy} = twisting curvature in the laminate

z = distance from the mid-plane in the thickness direction.

The mid-surface strain and curvature are always assumed zero and not function of z. Integrations at mid-surface yields:

$$\begin{Bmatrix} N_{xx} \\ N_{yy} \\ N_{xy} \end{Bmatrix} = \sum_{k=1}^{n} \left\{ \begin{bmatrix} \bar{Q}_{11} & \bar{Q}_{12} & \bar{Q}_{16} \\ \bar{Q}_{12} & \bar{Q}_{22} & \bar{Q}_{26} \\ \bar{Q}_{16} & \bar{Q}_{26} & \bar{Q}_{66} \end{bmatrix} \begin{Bmatrix} \varepsilon_{xx}^0 \\ \varepsilon_{yy}^0 \\ \gamma_{xy}^0 \end{Bmatrix} (h_k - h_{k-1}) + \begin{bmatrix} \bar{Q}_{11} & \bar{Q}_{12} & \bar{Q}_{16} \\ \bar{Q}_{12} & \bar{Q}_{22} & \bar{Q}_{26} \\ \bar{Q}_{16} & \bar{Q}_{26} & \bar{Q}_{66} \end{bmatrix} \begin{Bmatrix} k_{xx} \\ k_{yy} \\ k_{xy} \end{Bmatrix} \frac{1}{2}(h_k^2 - h_{k-1}^2) \right\} \quad (32)$$

$$\begin{Bmatrix} M_{xx} \\ M_{yy} \\ M_{xy} \end{Bmatrix} = \sum_{k=1}^{n} \left\{ \begin{bmatrix} \bar{Q}_{11} & \bar{Q}_{12} & \bar{Q}_{16} \\ \bar{Q}_{12} & \bar{Q}_{22} & \bar{Q}_{26} \\ \bar{Q}_{16} & \bar{Q}_{26} & \bar{Q}_{66} \end{bmatrix} \begin{Bmatrix} \varepsilon_{xx}^0 \\ \varepsilon_{yy}^0 \\ \gamma_{xy}^0 \end{Bmatrix} (h_k - h_{k-1}) + \begin{bmatrix} \bar{Q}_{11} & \bar{Q}_{12} & \bar{Q}_{16} \\ \bar{Q}_{12} & \bar{Q}_{22} & \bar{Q}_{26} \\ \bar{Q}_{16} & \bar{Q}_{26} & \bar{Q}_{66} \end{bmatrix} \begin{Bmatrix} k_{xx} \\ k_{yy} \\ k_{xy} \end{Bmatrix} \frac{1}{3}(h_k^3 - h_{k-1}^3) \right\} \quad (33)$$

$$\begin{Bmatrix} N_x \\ N_y \\ N_{xy} \\ M_x \\ M_y \\ M_{xy} \\ P_x \\ P_y \\ P_{xy} \end{Bmatrix} = \begin{bmatrix} A_{11} A_{12} A_{16} B_{11} B_{12} B_{16} E_{11}\, E_{12}\, E_{16} \\ A_{12} A_{22} A_{26} B_{12} B_{22} B_{26} E_{12}\, E_{22}\, E_{26} \\ A_{16} A_{26} A_{66} B_{16} B_{26} B_{66} E_{16}\, E_{26}\, E_{66} \\ B_{11} B_{12} B_{16} D_{11} D_{12} D_{16} F_{11}\, F_{12}\, F_{16} \\ B_{12} B_{22} B_{26} D_{12} D_{22} D_{26} F_{12}\, F_{22}\, F_{26} \\ B_{16} B_{26} B_{66} D_{16} D_{26} D_{66} F_{16}\, F_{26}\, F_{66} \\ E_{11} E_{12} E_{16} F_{11}\, F_{12}\, F_{12} H_{11} H_{12} H_{16} \\ E_{12} E_{22} E_{26} F_{12}\, F_{22}\, F_{26} H_{12} H_{22} H_{16} \\ E_{16} E_{26} E_{66} F_{16}\, F_{26}\, F_{66} H_{16} H_{26} H_{66} \end{bmatrix} \begin{Bmatrix} \epsilon_x^0 + L_n \epsilon_x^n \\ \epsilon_y^0 + L_n \epsilon_y^n \\ \gamma_y^0 + L_n \gamma_y^n \\ k_x^1 \\ k_y^1 \\ k_{xy}^1 \\ k_x^2 \\ k_y^2 \\ k_{xy}^2 \end{Bmatrix} \quad (34)$$

The laminate reduced transformed stiffness matrices and the ply thickness reference coordinate h_k can be combined to form new matrices. The element stiffness matrices: [A], [B], [D], [E], [F], and [H] may be written as:

$$A_{ij} = \sum_{k=1}^{n} [\bar{Q}_{ij}]_k (h_k - h_{k-1}) = \sum_{k=1}^{n} [\bar{Q}_{ij}]_k t_k,$$

$$B_{ij} = \frac{1}{2} \sum_{k=1}^{n} [\bar{Q}_{ij}]_k (h_k^2 - h_{k-1}^2), = \sum_{k=1}^{n} [\bar{Q}_{ij}]_k\, t_k \frac{(h_k + h_{k-1})}{2},$$

$$D_{ij} = \frac{1}{3} \sum_{k=1}^{n} [\bar{Q}_{ij}]_k (h_k^3 - h_{k-1}^3) = \frac{1}{3} \sum_{k=1}^{n} [\bar{Q}_{ij}]_k (t_k^3 + t\bar{z}_k{}^2),$$

$$E_{ij} = \frac{1}{4} \sum_{k=1}^{n} [\bar{Q}_{ij}]_k (h_k^4 - h_{k-1}^4) = \frac{1}{4} \sum_{k=1}^{n} [\bar{Q}_{ij}]_k (t_k^4 + t\bar{z}_k{}^3)$$

$$F_{ij} = \frac{1}{5} \sum_{k=1}^{n} [\bar{Q}_{ij}]_k (Z_K^5 - Z_{K-1}^5) = \frac{1}{5} \sum_{k=1}^{n} [\bar{Q}_{ij}]_k (t_k^5 + t\bar{z}_k{}^4)$$

$$H_{ij} = \frac{1}{7} \sum_{k=1}^{n} [\bar{Q}_{ij}]_k (Z_K^7 - Z_{K-1}^7) = \frac{1}{7} \sum_{k=1}^{n} [\bar{Q}_{ij}]_k (t_k^7 + t\bar{z}_k{}^6)$$

Where i, j =1, 2, 6; so stresses may be written as follows:

$$\sigma_x = \bar{Q}_{11}\epsilon_x^0 + \bar{Q}_{12}\epsilon_y^0 + \bar{Q}_{16}\gamma_y^0 + (\bar{Q}_{11}k_x^1 + \bar{Q}_{12}k_y^1 + \bar{Q}_{16}k_{xy}^1)z$$
$$+(\bar{Q}_{11}k_x^2 + \bar{Q}_{12}k_y^2 + \bar{Q}_{16}k_{xy}^2)z^3 + L_n(\bar{Q}_{11}\epsilon_x^n + \bar{Q}_{12}\epsilon_y^n + \bar{Q}_{16}\gamma_{xy}^n)$$
$$\sigma_y = \bar{Q}_{12}\epsilon_x^0 + \bar{Q}_{22}\epsilon_y^0 + \bar{Q}_{26}\gamma_y^0 + (\bar{Q}_{12}k_x^1 + \bar{Q}_{22}k_y^1 + \bar{Q}_{26}k_{xy}^1)z$$
$$+(\bar{Q}_{12}k_x^2 + \bar{Q}_{22}k_y^2 + \bar{Q}_{26}k_{xy}^2)z^3 + L_n(\bar{Q}_{12}\epsilon_x^n + \bar{Q}_{22}\epsilon_y^n + \bar{Q}_{26}\gamma_{xy}^n)$$
$$\sigma_{yz} = \bar{Q}_{44}(\gamma_{yz}^1 + z^2\gamma_{yz}^2) + \bar{Q}_{45}(\gamma_{xz}^1 + z^2\gamma_{xz}^2)$$
$$\sigma_{xz} = \bar{Q}_{45}(\gamma_{yz}^1 + z^2\gamma_{yz}^2) + \bar{Q}_{55}(\gamma_{xz}^1 + z^2\gamma_{xz}^2)$$
$$\sigma_{xy} = \bar{Q}_{16}\epsilon_x^0 + \bar{Q}_{26}\epsilon_y^0 + \bar{Q}_{66}\gamma_{xy}^0 + (\bar{Q}_{16}k_x^1 + \bar{Q}_{26}k_y^1 + \bar{Q}_{66}k_{xy}^1)z +$$
$$(\bar{Q}_{16}k_x^2 + \bar{Q}_{26}k_y^2 + \bar{Q}_{66}k_{xy}^2)z^3 + L_n(\bar{Q}_{16}k_x^n + \bar{Q}_{26}k_y^n + \bar{Q}_{66}\gamma_{xy}^n)z^3$$

Applying unidirectional load in x-axis direction, the matrix of Eq. (34) becomes,

$$\begin{Bmatrix} N_x \\ 0 \\ 0 \\ 0 \\ 0 \\ 0 \\ 0 \\ 0 \\ 0 \end{Bmatrix} = \begin{bmatrix} A_{11} A_{12} A_{16} B_{11} B_{12} B_{16} E_{11}\, E_{12}\, E_{16} \\ A_{12} A_{22} A_{26} B_{12} B_{22} B_{26} E_{12}\, E_{22}\, E_{26} \\ A_{16} A_{26} A_{66} B_{16} B_{26} B_{66} E_{16}\, E_{26}\, E_{66} \\ B_{11} B_{12} B_{16} D_{11} D_{12} D_{16} F_{11}\, F_{12}\, F_{16} \\ B_{12} B_{22} B_{26} D_{12} D_{22} D_{26} F_{12}\, F_{22}\, F_{26} \\ B_{16} B_{26} B_{66} D_{16} D_{26} D_{66} F_{16}\, F_{26}\, F_{66} \\ E_{11} E_{12} E_{16} F_{11}\, F_{12}\, F_{12} H_{11} H_{12} H_{16} \\ E_{12} E_{22} E_{26} F_{12}\, F_{22}\, F_{26} H_{12} H_{22} H_{16} \\ E_{16} E_{26} E_{66} F_{16}\, F_{26}\, F_{66} H_{16} H_{26} H_{66} \end{bmatrix} \begin{Bmatrix} \epsilon_x^0 + L_n \epsilon_x^n \\ \epsilon_y^0 + L_n \epsilon_y^n \\ \gamma_y^0 + L_n \gamma_y^n \\ k_x^1 \\ k_y^1 \\ k_{xy}^1 \\ k_x^2 \\ k_y^2 \\ k_{xy}^2 \end{Bmatrix} \quad (35)$$

Using the relation

$$(h_k^3 - h_{k-1}^3) = [(h_k - h_{k-1})^3 + 3(h_k - h_{k-1})(h_k + h_{k-1})^2 - 3(h_k^3 - h_{k-1}^3)]$$

International Journal of Scientific Engineering and Science
Volume 5, Issue 7, pp. 58-73, 2021. ISSN (Online): 2456-7361

$= t_k^3 + 12t\bar{z}_k^{\,2}$

Where h_{j-1}; distance from the mid-plane to the top of the j^{th} lamina, h_j: distance from the mid-plane to the bottom of the j^{th} lamina, and thickness of the k^{th} lamina denoted by t_k and $\bar{z}_k = \frac{(h_k + h_{k-1})}{2}$, and putting Ln =0.

Due to inherent heterogeneity, anisotropy, complicated geometries, and variety of loading, the in-plane forces cause out-of-plane deformations. Components of such laminates may be obtained by referring stress and strain components. The principal system of material coordinates (1, 2, 3) related to an arbitrary coordinate system (x, y, z) by the transformation relations as shown in Figure 9.

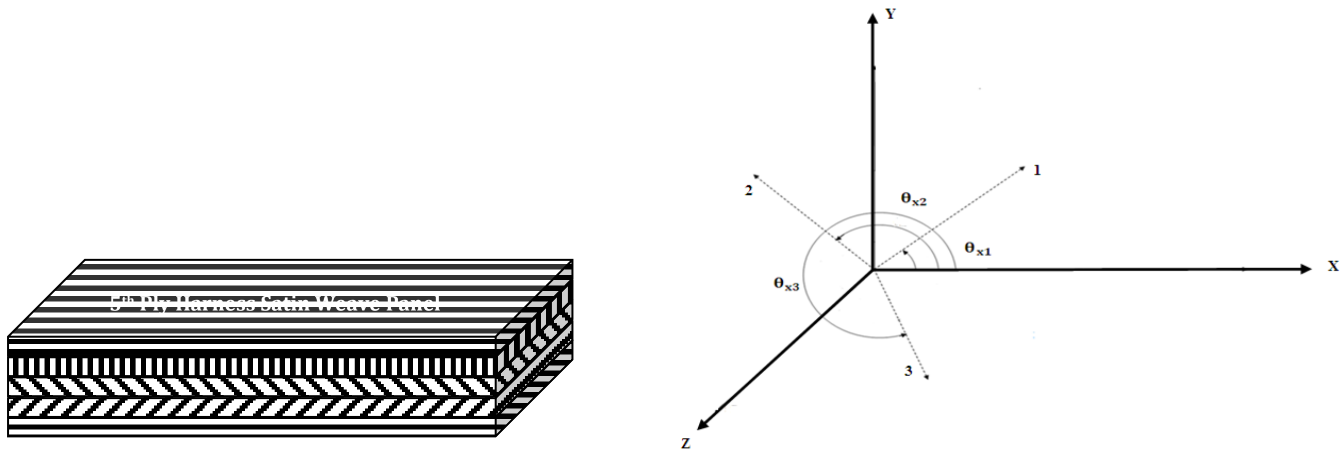

a) b)

Figure 9: a) 3-D panel, b) Coordinate systems referred to 3D transformation relations

Stress and strain components in local-coordinates may be related to the corresponding components in global-coordinates along with transformation matrix as follows:

$$\begin{Bmatrix} \sigma_{11} \\ \sigma_{22} \\ \sigma_{33} \\ \tau_{23} \\ \tau_{13} \\ \tau_{12} \end{Bmatrix} = \left[T_{ij}\right] \begin{Bmatrix} \sigma_{xx} \\ \sigma_{yy} \\ \sigma_{zz} \\ \tau_{yz} \\ \tau_{xz} \\ \tau_{xy} \end{Bmatrix} \quad \textbf{(36)}$$

$$\begin{Bmatrix} \varepsilon_{11} \\ \varepsilon_{22} \\ \varepsilon_{33} \\ \frac{1}{2}\gamma_{23} \\ \frac{1}{2}\gamma_{13} \\ \frac{1}{2}\gamma_{12} \end{Bmatrix} = \left[T_{ij}\right] \begin{Bmatrix} \varepsilon_{xx} \\ \varepsilon_{yy} \\ \varepsilon_{zz} \\ \frac{1}{2}\gamma_{yz} \\ \frac{1}{2}\gamma_{xz} \\ \frac{1}{2}\gamma_{xy} \end{Bmatrix} \quad \textbf{(37)}$$

Where transformation matrix is given as,

$$T_{ij} = \begin{bmatrix} m_1^2 & n_1^2 & p_1^2 & 2n_1p_1 & 2m_1p_1 & 2n_1m_1 \\ m_2^2 & n_2^2 & p_2^2 & 2n_2p_2 & 2m_2p_2 & 2n_2m_2 \\ m_3^2 & n_3^2 & p_3^2 & 2n_3p_3 & 2m_3p_3 & 2n_3m_3 \\ m_2m_3 & n_2n_3 & p_2p_3 & n_2p_3 + p_2n_3 & p_2m_3 + p_3m_2 & m_2n_3 + n_2m_3 \\ m_1m_3 & n_1n_3 & p_1p_3 & n_3p_1 + p_3n_1 & m_1p_3 + p_1m_3 & n_1m_3 + m_1n_3 \\ m_2m_1 & n_2n_1 & p_2p_1 & n_1p_2 + p_1n_2 & m_2p_1 + p_2m_1 & n_2m_1 + m_2n_1 \end{bmatrix}$$

The transformation relations for angles ($\theta_{x1}\ \theta_{x2}\ \theta_{x3}$) measured from x-axis to axis 1-, 2-, 3-axes in terms of direction cosines m_i, n_i and p_i are given as:

$m_1 = \cos\theta_{x1}$; $m_2 = \cos\theta_{x2}$; $m_3 = \cos\theta_{x3}$

$n_1 = \cos\theta_{y1}$; $n_2 = \cos\theta_{y2\,;}$ $n_3 = \cos\theta_{y3}$

$p_1 = \cos\theta_{z1}$; $p_2 = \cos\theta_{z2;}$ $p_3 = \cos\theta_{z3}$

To transform the lamina stiffness matrix into a global form using the transformed coefficient with different angles and thickness of each layer, the transformed stiffness matrices can be calculated. Denoting q, r, and s as contractions of the subscripts y-z, z-x, and x-y the following 3D formulations for coefficients of the reduced stiffen matrices:

International Journal of Scientific Engineering and Science
Volume 5, Issue 7, pp. 58-73, 2021. ISSN (Online): 2456-7361

$$Q_{xx} = m_1^4Q_{11} + 2m_1^2m_2^2Q_{12} + 2m_1^2m_3^2Q_{13} + m_2^4Q_{22} + 2m_3^2m_2^2Q_{23} + m_3^4Q_{33} + 4m_3^2m_2^2Q_{44} + 4m_1^2m_3^2C_{55} + 4m_1^2m_3^2C_{66} \quad (38)$$

$$Q_{xy} = m_1^2m_2^2Q_{11} + (m_1^2n_2^2 + m_2^2n_1^2)Q_{12} + (m_1^2n_3^2 + m_3^2n_1^2m_1^2)Q_{13} + m_2^2n_2^2Q_{22} + (m_2^2n_3^2 + m_3^2n_2^2)Q_{23} + m_3^2n_3^2Q_{33} + 4m_2m_3n_2n_3Q_{44} + 4m_1m_3n_1n_3C_{55} + 4m_2m_1n_2n_1C_{66} \quad (39)$$

$$Q_{xz} = m_1^2p_1^2Q_{11} + (m_1^2p_2^2 + m_2^2p_1^2m_1^2)Q_{12} + (m_1^2p_3^2 + m_3^2p_1^2)Q_{13} + m_2^2p_2^2Q_{22} + (m_2^2p_3^2 + m_3^2p_2^2)Q_{23} + m_3^2p_3^2Q_{33} + 4m_2m_3p_2p_3Q_{44} + 4m_1m_3p_1p_3C_{55} + 4m_2m_1p_2p_1C_{66} \quad (40)$$

$$Q_{xq} = [2m_1^2n_1p_1Q_{11} + (2m_1^2n_2p_2 + 2m_2^2n_1p_1)Q_{12} + (2m_1^2n_3p_3 + 2m_3^2n_1p_1)Q_{13} + 2m_2^2n_2p_2Q_{22} + (2m_2^2n_3p_3 + 2m_3^2n_2p_2)Q_{23} + 2m_3^2n_3p_3Q_{33} + 4m_2m_3(n_2p_3 + n_3p_2)Q_{44} + 4m_1m_3(n_1p_3 + n_3p_1)C_{55} + 4m_2m_1(n_1p_2 + p_1n_2)C_{66}]/2 \quad (41)$$

$$Q_{xr} = [2m_1^3p_1Q_{11} + 2m_2m_1(m_1p_2 + p_1m_2)Q_{12} + 2m_1m_3(m_1p_3 + m_3p_1)Q_{13} + 2m_2^3p_2Q_{22} + 2m_2m_3(m_2p_3 + m_3p_2)Q_{23} + 2m_3^3p_32m_3^3p_3Q_{33} + 4m_2m_3(m_2p_3 + m_3p_2)Q_{44} + 4m_1m_3(m_1p_3 + m_3p_1)C_{55} + 4m_2m_1(m_1p_2 + p_1m_2)C_{66}]/2 \quad (42)$$

$$Q_{xs} = [2m_1^3n_1Q_{11} + 2m_2m_1(m_1n_2 + n_1m_2)Q_{12} + 2m_1m_3(m_1n_3 + m_3n_1)Q_{13} + 2m_2^3n_2Q_{22} + 2m_2m_3(m_2n_3 + m_3n_2)Q_{23} + 2m_3^3n_3Q_{33} + 4m_2m_3(m_2n_3 + m_3n_2)Q_{44} + 4m_1m_3(m_1n_3 + m_3n_1)C_{55} + 4m_2m_1(m_1n_2 + n_1m_2)C_{66}]/2 \quad (43)$$

$$Q_{yy} = n_1^4Q_{11} + 2n_1^2n_2^2Q_{12} + 2n_1^2n_3^2Q_{13} + n_2^4Q_{22} + n_3^2n_2^2Q_{23} + n_3^4Q_{33} + 4n_3^2n_2^2Q_{44} + 4n_1^2n_3^2C_{55} + 4n_1^2n_2^2C_{66} \quad (44)$$

$$Q_{yz} = n_1^2p_1^2Q_{11} + (n_1^2p_2^2 + n_2^2p_1^2)Q_{12} + (n_1^2p_3^2 + n_3^2p_1^2)Q_{13} + n_2^2p_2^2Q_{22} + (n_2^2p_3^2 + n_3^2p_2^2)Q_{23} + n_3^2p_3^2Q_{33} + 4n_2n_3p_2p_3Q_{44} + 4n_1n_3p_1p_3C_{55} + 4n_1n_2p_1p_2C_{66} \quad (45)$$

$$Q_{yq} = [2n_1^3p_1Q_{11} + 2n_2n_1(n_1p_2 + p_1n_2)Q_{12} + 2n_3n_1(n_1p_3 + p_1n_3)Q_{13} + 2n_2^3p_2Q_{22} + 2n_3n_2(n_2p_3 + p_2n_3)Q_{23} + 2n_3^3p_3Q_{33} + 4n_3n_2(n_2p_3 + p_2n_3)Q_{44} + 4n_3n_1(n_1p_3 + p_1n_3)C_{55} + 4n_2n_1(n_1p_2 + p_1n_2)C_{66]/2} \quad (46)$$

$$Q_{yr} = [2n_1^2m_1p_1Q_{11} + 2n_2n_1(n_1p_2 + p_1n_2)Q_{12} + (2n_3^2m_1p_1 + 2n_1^2m_3p_3)Q_{13} + 2n_2^2m_2p_2Q_{22} + (2n_3^2m_2p_2 + 2n_2^2m_3p_3)Q_{23} + 2n_3^2m_3p_3Q_{33} + 4n_2n_3(m_2p_3 + p_2m_3)Q_{44} + 4n_1n_3(m_1p_3 + p_1m_3)C_{55} + 4n_2n_1(m_1p_2 + p_1m_2)C_{66]/2} \quad (47)$$

$$Q_{ys} = [2n_1^3m_1Q_{11} + 2n_2n_1(m_1n_2 + n_1m_2)Q_{12} + 2n_1n_3(m_1n_3 + n_1m_3)Q_{13} + 2n_2^3m_2Q_{22} + 2n_2n_3(m_2\,n_3 + n_2m_3)Q_{23} + 2m_3^3n_3Q_{33} + 4n_2n_3(m_2n_3 + n_2m_3)Q_{44} + 4n_1n_3(m_1n_3 + n_1m_3)C_{55} + 4n_2n_1(m_1n_2 + n_1m_2)C_{66]/2} \quad (48)$$

$$Q_{zz} = p_1^4Q_{11} + 2p_1^2p_2^2Q_{12} + 2p_1^2p_3^2Q_{13} + p_2^4Q_{22} + p_3^2p_2^2Q_{23} + p_3^4Q_{33} + 4p_3^2p_2^2Q_{44} + 4p_1^2p_3^2C_{55} + 4p_1^2p_2^2C_{66} \quad (49)$$

$$Q_{zq} = [2p_1^3n_1Q_{11} + 2p_2p_1(n_1p_2 + p_1n_2)Q_{12} + 2p_3p_1(n_1p_3 + p_1n_3)Q_{13} + 2p_2^3n_2Q_{22} + 2p_2p_3(n_3p_2 + p_3n_2)Q_{23} + 2p_3^3n_3Q_{33} + 4p_2p_3(n_3p_2 + p_3n_2)Q_{44} + 4p_3p_1(n_1p_3 + p_1n_3)C_{55} + 4p_2p_1(n_1p_2 + p_1n_2)C_{66]/2} \quad (50)$$

$$Q_{zr} = [2p_1^3m_1Q_{11} + 2p_2p_1(m_1p_2 + p_1m_2)Q_{12} + 2p_3p_1(m_1p_3 + p_1m_3)Q_{13} + 2p_2^3m_2Q_{22} + 2p_2p_3(m_3p_2 + p_3m_2)Q_{23} + 2p_3^3m_3Q_{33} + 4p_2p_3(m_3p_2 + p_3m_2)Q_{44} + 4p_3p_1(m_1p_3 + p_1m_3)C_{55} + 4p_2p_1(m_1p_2 + p_1m_2)C_{66}]/2 \quad (51)$$

$$Q_{zs} = [2p_1^2m_1n_1Q_{11} + (2p_2^2m_1n_1 + 2p_1^2m_2n_2)Q_{12} + (2p_3^2m_1n_1 + 2p_1^2m_3n_3)Q_{13} + 2p_2^2m_2n_2Q_{22} + (2p_3^2m_2n_2 + 2p_2^2m_3n_3)Q_{23} + 2p_3^2m_3n_3Q_{33} + 4p_2p_3(m_3n_2 + n_3m_2)Q_{44} + 4p_3p_1(m_1n_3 + n_1m_3)C_{55} + 4p_2p_1(m_1n_2 + n_1m_2)C_{66]/2} \quad (52)$$

$$Q_{qq} = [4n_1^2p_1^2Q_{11} + 8p_1n_1p_2n_2Q_{12} + 8p_1n_1p_3n_3Q_{13} + 4n_2^2p_2^2Q_{22} + 8p_2n_2p_3n_3Q_{23} + 4n_3^2p_3^2Q_{33} + 4(p_3n_2 + n_3p_2)^2Q_{44} + 4(p_3n_1 + n_3p_1)^2C_{55} + 4(p_1n_2 + n_1p_2)^2C_{66]/4} \quad (53)$$

$$Q_{qr} = [4p_1^2m_1n_1Q_{11} + 4p_1p_2\,(m_1n_2 + n_1m_2)Q_{12} + 4p_1p_3\,(m_1n_3 + n_1m_3)Q_{13} + 4p_2^2m_2n_2Q_{22} + 4p_3p_2\,(m_3n_2 + n_3m_2)Q_{23} + 4p_3^2m_3n_3Q_{33} + 4(p_3n_2 + n_3p_2)(m_3p_2 + p_3m_2)Q_{44} + 4(m_3p_1 + p_3m_1)(p_3n_1 + n_3p_1)C_{55} + 4(p_1n_2 + n_1p_2)(m_1p_2 + p_1m_2)C_{66]/4} \quad (54)$$

$$Q_{qs} = [4n_1^2m_1p_1Q_{11} + 4n_1n_2\,(m_1p_2 + p_1m_2)Q_{12} + 4n_1n_3\,(m_1p_3 + p_1m_3)Q_{13} + 2n_2^2m_2p_2Q_{22} + 4n_3n_2\,(m_3p_2 + p_3m_2)Q_{23} + 4n_3^2m_3p_3Q_{33} + 4(p_3n_2 + n_3p_2)(m_3n_2 + n_3m_2)Q_{44} + 4(p_3n_1 + n_3p_1)(m_3n_1 + n_3m_1)C_{55} + 4(p_1n_2 + n_1p_2)(m_1n_2 + n_1m_2)C_{66}]/4 \quad (55)$$

$$Q_{rr} = [4m_1^2p_1^2Q_{11} + 8p_1m_1p_2m_2Q_{12} + 8p_1m_1p_3m_3Q_{13} + 4m_2^2p_2^2Q_{22} + 8p_2m_2p_3m_3Q_{23} + 4m_3^2p_3^2Q_{33} + 4(p_3m_2 + m_3p_2)^2Q_{44} + 4(p_3m_1 + m_3p_1)^2C_{55} + 4(p_1m_2 + m_1p_2)^2C_{66}]/4 \quad (56)$$

$$Q_{rs} = [4m_1^2n_1p_1Q_{11} + 4m_1m_2\,(n_1p_2 + p_1n_2)Q_{12} + 4m_1m_3\,(n_1p_3 + p_1n_3)Q_{13} + 4m_2^2p_2n_2Q_{22} + 4m_3m_2\,(n_3p_2 + p_3n_2)Q_{23} + 4m_3^2\,p_3n_3Q_{33} + 4(p_3m_2 + m_3p_2)(m_3n_2 + n_3m_2)Q_{44} + 4(p_3m_1 + m_3p_1)(m_3n_1 + n_3m_1)C_{55} + 4(p_1m_2 + m_1p_2)(m_1n_2 + n_1m_2)C_{66}]/4 \quad (57)$$

$$Q_{ss} = [4m_1^2n_1^2Q_{11} + 8n_1m_1n_2m_2Q_{12} + 8n_1m_1n_3m_3Q_{13} + 4n_2^2m_2^2Q_{22} + 8n_2m_2n_3m_3Q_{23} + 4m_3^2n_3^2Q_{33} + 4(n_3m_2 + m_3n_2)^2Q_{44} + 4(n_3m_1 + m_3n_1)^2C_{55} + 4(n_1m_2 + m_1n_2)^2C_{66}]/4 \quad (58)$$

The mathematical formulations may be utilised to formulate effective mechanical properties of laminated structural beam/plate panels of thickness H consisting of N plies rotated at angles θ_i:

$$\bar{E}_1 = \frac{1}{HN}\sum_{i=0}^{N} E_1(\theta_i) \quad (59)$$

$$\bar{E}_2 = \frac{1}{HN}\sum_{i=0}^{N} E_2(\theta_i) \quad (60)$$

$$\bar{G}_{12} = \frac{1}{HN}\sum_{i=0}^{N} G_{12}(\theta_i) \quad \textbf{(61)}$$
$$\bar{\nu}_{12} = \frac{1}{HN}\sum_{i=0}^{N} \nu_{12}(\theta_i) \quad \textbf{(62)}$$
$$\bar{\nu}_{21} = \frac{1}{HN}\sum_{i=0}^{N} \nu_{21}(\theta_i) \quad \textbf{(63)}$$

III. RESULTS AND DISCUSSIONS

Mathematical formulations relevant to the current study were selected out of the formulations presented in the Section2.3 above. Three-dimensional formulations were selected to program and implement in MATLAB^{TM} software to approximate the mechanical properties (elastic constants) as presented in Table 4, Table 5, and

Table 6. The coded programs were executed to predict effective mechanical properties of laminated structural beam/plate panels of thickness H (8-ply of 2.4 mm; 16-ply of 4.8 mm; and 24-ply of 7.2 mm thickness laminates) made of N plies as shown in Figure 1 with material properties provided in Table 1. Extensive data for mechanical properties (Young's modulus, shear modulus, and Poisson's ratios) from axis-aligned and rotated beam panels through simulations of tensile, shear, and bending tests, and effective were recorded. Selected data were plotted as functions for the four mechanical properties against ply orientation angles range: $-\pi/_2 \le \theta \le \pi/_2$ at the step difference of 10^0 depicted in Figure 10, Figure 11, Figure 12, and Figure 13. Selected quantities out of simulated results illustrated in Table 7 were compared against the data available in Table 1 and reference [14] and found to be within good agreement. Mechanical properties (elastic constants) are presented in Table 7 are independent, so the presented elastic constants were considered to be parallel in fibre directions in all cases.

Table 4: Computer program to predict mechanical properties

```
Clear
clc
e11=230;e22=23;neu12=0.2;g12=88;
diaryElastic_Constants.out
fprintf('====== Angle and Elastic constants ======\n'); fprintf(' ----------------------\n\n');
fprintf('Angle   \tExx       v12       Eyy Gxy \n');
 fprintf('=====  \t======= \t======= \t=======     =======    \n');
i=0;for ii = -90:10:90;i=i+1; ex1(i) = Ex(e11,e22, neu12, g12, ii);
neux1(i) = NUxy(e11,e22, neu12, g12, ii);ey2(i) = Ey(e11,e22, neu12, g12, ii);
%neuy2(i) = NUyx(e11,e22, neu12, g12, ii)
gxy(i) = Gxy(e11,e22, neu12, g12, ii);
fprintf('%2d \t\t%5.2f\t\t\t%5.2f\t\t\t%5.2f\t\t\t%5.2f\n',ii, ex1(i),neux1(i),ey2(i), gxy(i))
end
x=[-90 -80 -70 -60 -50 -40 -30 -20 -10 0 10 20 30 40 50 60 70 80 90];
ex=[23 24.28 28.61 37.69 55.41 88.86 143.52 200.83 226.73 230 226.73 200.83 143.52 88.86 55.41 37.69 28.61 24.28 23];
neu=[0.02 -0.01 -0.08 -0.18 -0.29 -0.39 -0.42 -0.32 -0.04 0.2 -0.04 -0.32 -0.42 -0.39 -0.29 -0.18 -0.08 -0.01 0.02];
ey=[230 252.98 297.4 247.96 134.08 70.16 42.38 30 24.56 23 24.56 30 42.38 70.16 134.08 247.96 297.4 252.98 230];
gxy=[88 63.16 36.84 24.99 20.66 20.66 24.99 36.84 63.16 88 63.16 36.84 24.99 20.66 20.66 24.99 36.84 63.16 88];
subplot(x,ex);xlabel('Angle,\theta(degree)');ylabel('E_{xx}');
title('Elasitic modulus Exx v Rotation'); subplot(x,neu,2);xlabel('Angle, \theta (degree)');ylabel('\neu_{12}');
title('Subplot 2 Poisson ratios');subplot(x,ey,3); xlabel('Angle, \theta (degree)');ylabel('E_{yy}');
title('Subplot 3 Elastic modulus Eyy');subplot(x,gxy,4); xlabel('Angle, \theta (degree)');ylabel('G_{xy}');
title('Subplot 4 Shear modulus Gxy');
diary off
e11=59.14;e22=59.14;nu12=0.2;g12=10.0;
diaryElastic_Constants.out
fprintf('====== Angle and Elastic constants ======\n'); fprintf('     ----------------------\n\n')
fprintf('Angle   \tExx       v12       EyyGxy \n');
 fprintf('=====  \t======= \t======= \t=======     ========    \n');
i=0;for ii = -90:10:90;i=i+1;ex1(i) = Ex(e11,e22, neu12, g12, ii); neux1(i) = NUxy(e11,e22, neu12, g12, ii);
ey2(i) = Ey(e11,e22, neu12, g12, ii);
%neuy2(i) = NUyx(e11,e22, neu12, g12, ii) gxy(i) = Gxy(e11,e22, neu12, g12, ii);
fprintf('%2d \t\t%5.2f\t\t\t%5.2f\t\t\t%5.2f\t\t\t%5.2f\n',ii, ex1(i),neux1(i),ey2(i), gxy(i)); end
x=[-90 -80 -70 -60 -50 -40 -30 -20 -10 0 10 20 30 40 50 60 70 80 90];
ey=[230 252.98 297.4 247.96 134.08 70.16 2.38 30 24.56 23 24.56 30 42.38 70.16 134.08 247.96 297.4 252.98 230];
plot(x,ey); xlabel('Angle, \theta (degree)'); ylabel('E_{yy}'); title('Elastic modulus Eyy');
diary off
```

Table 5: Computer program for mechanical properties by tensile-bending

```
Clear
clc
function y = Ex(E1,E2,NU12,G12,theta)
m = cos(theta*pi/180);n = sin(theta*pi/180);denom = m^4 + (E1/G12 - 2*NU12)*n*n*m*m + (E1/E2)*n^4;y = E1/denom;
function y = NUxy(E1,E2,NU12,G12,theta);%NUxy This function returns Poisson's ratio % NUxy in the global
m = cos(theta*pi/180);n = sin(theta*pi/180);denom = m^4 + (E1/G12 - 2*NU12)*n*n*m*m + (E1/E2)*n*n;
numer=NU12*(n^4 + m^4)-(1+E1/E2-E1/G12)*n*n*m*m;y=numer/denom;
```

Volume 5, Issue 7, pp. 58-73, 2021.
ISSN (Online): 2456-7361

```
function y = Ey(E1,E2,NU21,G12,theta)
m = cos(theta*pi/180);n = sin(theta*pi/180); denom = m^4 + (E2/G12 - 2*NU21)*n*n*m*m + (E2/E1)*n^4;y = E2/denom;
function y = Gbarxy(A,H);a = inv(A); y = 1/(H*a(3,3));
function y = Gxy(E1,E2,NU12,G12,theta)
m = cos(theta*pi/180);n = sin(theta*pi/180);denom = n^4 + m^4 + 2*(2*G12*(1 + 2*NU12)/E1 + 2*G12/E2 - 1)*n*n*m*m;
y = G12/denom;
function y = NUbarxy(A,H);a = inv(A);y = -a(1,2)/a(1,1);function y = NUxy(E1,E2,NU12,G12,theta)
m = cos(theta*pi/180);n = sin(theta*pi/180);denom = m^4 + (E1/G12 - 2*NU12)*n*n*m*m + (E1/E2)*n*n;
numer = NU12*(n^4 + m^4) - (1 + E1/E2 - E1/G12)*n*n*m*m;y = numer/denom;
function y = NUyx(E1,E2,NU21,G12,theta)
m = cos(theta*pi/180);n = sin(theta*pi/180);denom = m^4 + (E2/G12 - 2*NU21)*n*n*m*m + (E2/E1)*n*n;
numer = NU21*(n^4 + m^4) - (1 + E2/E1 - E2/G12)*n*n*m*m;y = numer/denom;e11=230;e22=23;neu12=0.2;g12=88;
diary Elastic_Constants.out
fprintf('====== Angle and Elastic constants ======\n');fprintf('      ----------------------\n\n')
fprintf('Angle   \tExx       v12       EyyGxy \n');fprintf('=====   \t=======  \t=======  \t=======     ========   \n');
i=0;for ii = -90:10:90;i=i+1;ex1(i) = Ex(e11,e22, neu12, g12, ii); neux1(i) = NUxy(e11,e22, neu12, g12, ii);ey2(i) = Ey(e11,e22, neu12, g12, ii);%neuy2(i) = NUyx(e11,e22, neu12, g12, ii)gxy(i) = Gxy(e11,e22, neu12, g12, ii);
fprintf('%2d \t\t%5.2f\t\t%5.2f\t\t%5.2f\t\t%5.2f\n',ii, ex1(i),neux1(i),ey2(i), gxy(i));end
x=[-90 -80 -70 -60 -50 -40 -30 -20 -10 0 10 20 30 40 50 60 70 80 90];
neu=[0.02 -0.01 -0.08 -0.18 -0.29 -0.39 -0.42 -0.32 -0.04 0.2 -0.04 -0.32 -0.42 -0.39 -0.29 -0.18 -0.08 -0.01 0.02];
plot(x,neu);xlabel('Angle, \theta (degree)');ylabel('\nu_{12}');diary off
function y = Qbar(Q,theta)
m = cos(theta*pi/180);n = sin(theta*pi/180);T = [m*m n*n 2*m*n ; n*n m*m -2*m*n ; -m*n m*n m*m-n*n];
Tinv = [m*m n*n -2*m*n ; n*n m*m 2*m*n ; m*n -m*n m*m-n*n];y = Tinv*Q*T;
function y = ReducedStiffness(E1,E2,NU12,G12)
NU21 = NU12*E2/E1;y = [E1/(1-NU12*NU21) NU12*E2/(1-NU12*NU21) 0 ;NU12*E2/(1-NU12*NU21) E2/(1-NU12*NU21) 0 ; 0 0 G12];e11=230;e22=23;neu12=0.2;g12=88; diaryElastic_Constants.out
fprintf('====== Angle and Elastic constants ======\n');fprintf('----------------------\n\n');fprintf('Angle\tExx v12    EyyGxy \n');fprintf('=====   \t=======  \t=======  \t=======  ==\n');i=0;for ii = -90:10:90;i=i+1;ex1(i) = Ex(e11,e22, neu12, g12, ii);neux1(i) = NUxy(e11,e22, neu12, g12, ii);ey2(i) = Ey(e11,e22, neu12, g12, ii);%neuy2(i) = NUyx(e11,e22, neu12, g12, ii)gxy(i) = Gxy(e11,e22, neu12, g12, ii); fprintf('%2d  \t\t%5.2f\t\t%5.2f\t\t%5.2f\t\t%5.2f\n',ii, ex1(i),neux1(i),ey2(i), gxy(i));end; x=[-90 -80 -70 -60 -50 -40 -30 -20 -10 0 10 20 30 40 50 60 70 80 90];
gxy=[88 63.16 36.84 24.99 20.66 20.66 24.99 36.84 63.16 88 63.16 36.84 24.99 20.66 20.66 24.99 36.84 63.16 88];
plot(x,gxy);xlabel('Angle, \theta (degree)');ylabel('G_{xy}'); title('Shear modulus Gxy');
diary off; e11=59.14;% in directions parallel and perpendicular to fibres e22= 6;% in any angle to fibre direction
nu12=0.2;N=8;e(1)=6;e(2)=e(1);e(3)=59.14;e(4)=e(3);sum =e(1);for k = 2:N/2;sum =sum +e(k)*(k^3-(k-1)^3);end
ex=8*sum/N^3;end
```

Table 6: Code for effective mechanical properties of 3-D panels

```
==========================================================
||      TO PREDICT EFFECTIVE ENGINEERING CONSTANTS   OF PANEL     ||
==========================================================
clear
clc
e11=58.8;e22=58.80;nu12=0.2;g12=10.0;Q=ReducedStiffness(e11,e22,nu12,g12);
Qbar1=Qbar(Q,0);Qbar2=Qbar(Q,90);Qbar3=Qbar(Q,45);Qbar4=Qbar(Q,-45);Qbar5=Qbar(Q,-45);Qbar6=Qbar(Q,45);
Qbar7=Qbar(Q,90);Qbar8=Qbar(Q,0);z1=-1.2;z2=-0.9;z3=-0.6;z4=-0.3;z5=0.00;z6=0.3;z7=0.6;z8=0.9;z9=1.12;
A=zeros(3,3);A=Amatrix(A,Qbar1,z1,z2);A=Amatrix(A,Qbar2,z2,z3);A=Amatrix(A,Qbar3,z3,z4);A=Amatrix(A,Qbar4,z4,z5);
A=Amatrix(A,Qbar5,z5,z6);A=Amatrix(A,Qbar6,z6,z7);A=Amatrix(A,Qbar7,z7,z8);A=Amatrix(A,Qbar8,z8,z9);a=A;B = zeros(3,3);
B = Bmatrix(B,Qbar1,z1,z2);B = Bmatrix(B,Qbar2,z2,z3);B = Bmatrix(B,Qbar3,z3,z4);B = Bmatrix(B,Qbar4,z4,z5);
B = Bmatrix(B,Qbar5,z5,z6);B = Bmatrix(B,Qbar6,z6,z7);B = Bmatrix(B,Qbar7,z7,z8);B = Bmatrix(B,Qbar8,z8,z9);b=B;
D = zeros(3,3);D = Dmatrix(D,Qbar1,z1,z2)D = Dmatrix(D,Qbar2,z2,z3);D = Dmatrix(D,Qbar3,z3,z4); D = Dmatrix(D,Qbar4,z4,z5)
D = Dmatrix(D,Qbar5,z5,z6);D = Dmatrix(D,Qbar6,z6,z7);D = Dmatrix(D,Qbar7,z7,z8);D = Dmatrix(D,Qbar8,z8,z9)
d=D;H=2.4;h=H;abd=[a(1,1) a(1,2) a(1,3) b(1,1) b(1,2) b(1,3);
a(2,1) a(2,2) a(2,3) b(2,1) b(2,2) b(2,3);a(3,1) a(3,2) a(3,3) b(3,1) b(3,2) b(3,3);b(1,1) b(1,2) b(1,3) d(1,1) d(1,2) d(1,3);
b(2,1) b(2,2) b(2,3) d(2,1) d(2,2) d(2,3);b(3,1) b(3,2) b(3,3) d(3,1) d(3,2) d(3,3)];bd=[ a(2,2) a(2,3) b(2,1) b(2,2) b(2,3);
a(3,2) a(3,3) b(3,1) b(3,2) b(3,3);b(1,2) b(1,3) d(1,1) d(1,2) d(1,3); b(2,2) b(2,3) d(2,1) d(2,2) d(2,3);b(3,2) b(3,3) d(3,1) d(3,2) d(3,3)];ab=det(abd)/det(bd);ex=abs(ab*1/h);
end
```

Volume 5, Issue 7, pp. 58-73, 2021.

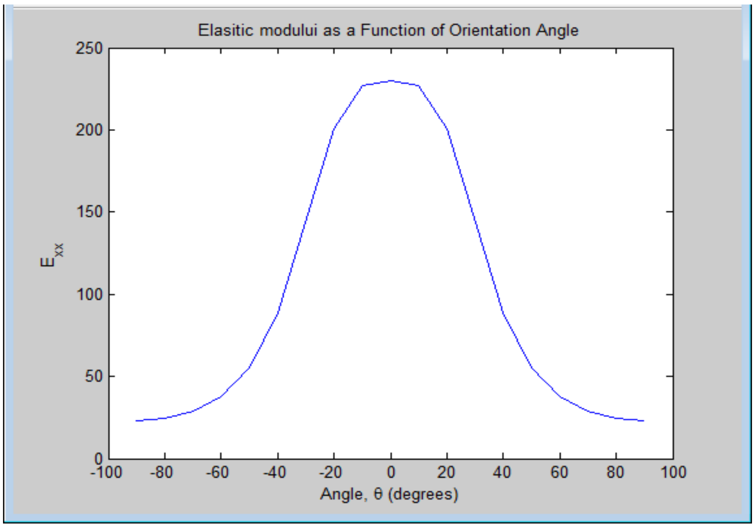

Figure 10: Elastic constants in parallel to fibre direction against orientation angles

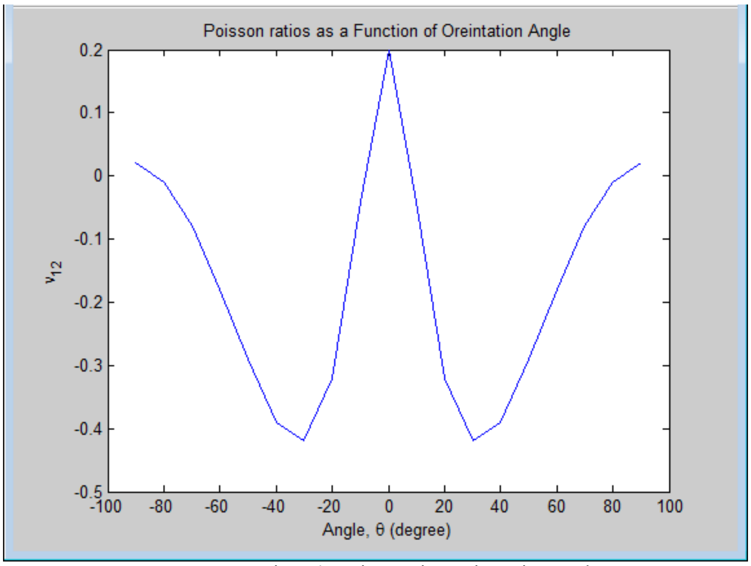

Figure 11: Poisson’s ratios against orientation angle

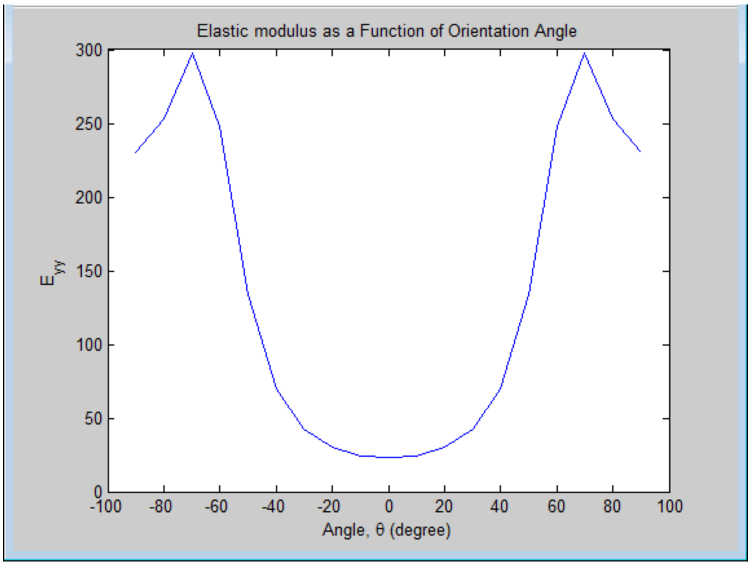

Figure 12: Elastic constants perpendicular to fibre against orientation angle

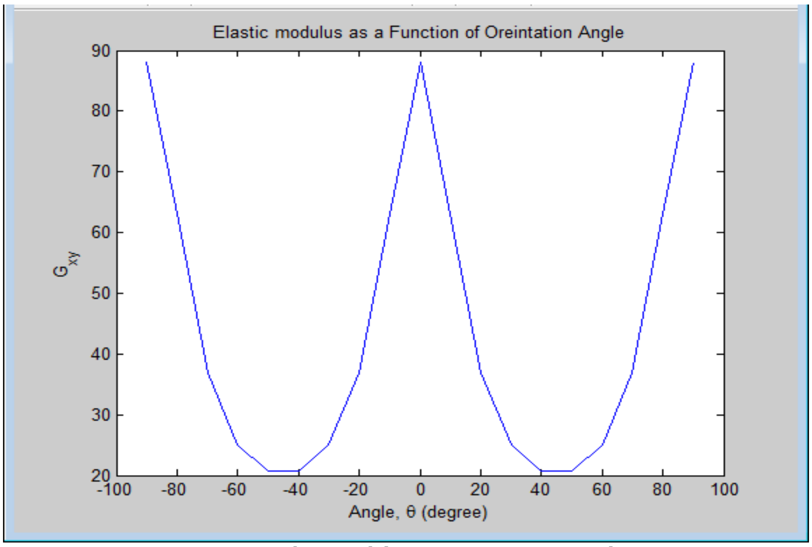

Figure 13: Shear modulus against orientation angle

Table 7: Simulation produced data

Young's modulus GPa		
8-Ply	16-Ply	24-Ply
56.5	46.6	45.8

IV. CONCLUSIONS

In this work, mechanical properties of carbon fibre-reinforced laminated composite panels were determined from experimental tests and micro-macro mechanics theory. Micro-macro mechanics laws were applied to systematically develop formulations from one-, two-, and three-dimensional panels. The following conclusions can be extracted from the study:

- Experimental tests were conducted to determine baseline for mechanical properties
- Micro-macro mechanics based mathematical formulations were developed and implemented into commercial software MATLAB™ to predict the mechanical properties
- Mechanical properties were determined from theoretical calculations considering influence from deformations due to coupling in global coordinate were considered
- Simulation produced results were compared and validated against the values obtained by tensile and flexural tests and found to be within acceptable deviations (±10%).

Based on acceptable comparisons of the results, the study proposed that micro-macro mechanics laws utilising in-plane material properties and stress-strain relations could be useful to effectively predict mechanical properties influenced by coupling deformation parameters.

REFERENCES

[1] Daniel B. Miracle and Steven L. Donaldson 'Composite Materials Handbook Volume 2. Polymer Matrix Composites Materials Properties' Book, Department of Defense Handbook, 1999.
[2] Jang-Kyo Kim and Yiu-Wing Mai 'Engineered Interfaces in Fiber Reinforced Composites' Book, Elsevier Science Ltd, 1998.
[3] Liyong Tong, Adrian P. Mouritz and Michael K. Bannister '3D Fibre Reinforced Polymer Composites' Book, Elsevier Science Ltd, 2002.
[4] Baker AA, Dutton S, Kelly D. Composite materials for aircraft structures. AIAA (Second Edition), USA, 2004.
[5] Morgan P. Carbon Fibres and their composites. Taylor & Francis, Boca Raton, USA, 2005.
[6] Ashby MF. Materials Selection in Mechanical Design (Third Edition), Butterworth-Heinemann, 2005.
[7] Barbero EJ. Introduction to composite materials design, (Second Edition), CRC Press Taylor & Francis Group, ISBN 978-1-4200-7915-9, USA, 2010.
[8] Abdalla F. H., Megat M. H., Sapuan M. S. and B. B. Sahari. Determination of Volume Fraction Values of filament Wound Glass and Carbon Fiber Reinforced Composites. ARPN Journal of Engineering and Applied Sciences, Vol. 3, No. 4, pp. 7-11, 2008.
[9] John EL, XiaowenY, Mark IJ. Characterisation of voids in fibre reinforced composite materials. NDT&E International 2012;46:122–127.
[10] Standard Test Methods 'D3039/D03039M' for Tensile Properties of Polymer Composite Materials. Annual Book of ASTM Standards, Vol. 15, 1995.
[11] Yang B, Kozey V, Adanur S, Kumar S. Bending, compression, and shear behaviour of woven glass fibre- epoxy composites. Composites: Part B 2000;31:715-21.
[12] Emilia S, Nicolai B and Paul B. Mechanical characteristics of composite materials obtained by different technologies. Academic J Manufactur Eng 2001;9(3):100-105.
[13] Hussain SA, Reddy SB and V, and Reddy VN. Prediction of elastic properties of FRP composite lamina for longitudinal loading. Asian Research Publishing Network (ARPN) 2008;3(6):70-75.
[14] Farooq U, Myler P. Efficient determination of mechanical properties of carbon fibre-reinforced laminated composite panels. I Journal of Engineering and Applied Sciences Asian Research Publishing Network (ARPN) 2017;12(5):1375-92.
[15] Ali S. Humod and Muhannad Al_Waily 'Experimental and Analytical Study of Tensile Properties for Hybrid Composite Material' The Iraqi Journal for Mechanical and Material Engineering 2010;(1):11-22.

[16] Keshavamurthy YC, Nanjundaradhya NV, Ramesh SS, Kulkarni RS. Investigation of tensile properties of fibre reinforced angle ply laminated composites. Int J Emerg Technol Adv Eng 2012;2(4):700-703.
[17] Altaf HS, PandurangaduV, Amba PRG. Prediction of elastic constants of carbon T300/ epoxy composite using soft computing. Int J Inn Research in Sci Eng Technol 2013;2(7): 2762-2770.
[18] Liang JZ. Predictions of Young's modulus of short inorganic fibre reinforced polymer composites. Composites: Part B 2012;2001-12.
[19] Bradley LR. Mechanical testing and modelling of carbon–carbon composites for aircraft disc brakes. PhD thesis, University of Bath, UK 2003.
[20] Konrad Gliesche, Tamara Hubner, Holger Orawetz. Investigations of in-plane shear properties of $\pm 45^0$ carbon/epoxy composites using tensile testing and optical deformation analysis. Compos Sci Technol 2005;65:163-171.
[21] Bradley LR, Bowen CR, McEnaney B, Johnson LR. Shear properties of a carbon/carbon composite with non-woven felt and continuous fibre reinforcement layers. Carbon 2007;45:2178–2187.
[22] Nicolaie Dan Cristescu, Eduard-Marius Craciun, and Eugen Soos 'Mechanics of Elastic Composites' Book, Chapman and Hall/CRC, 2004.
[23] Irina P, Cristina M, Constant I. The determination of Young modulus for cfrp using three point bending tests at different span lengths. Scientific Bulletin-University Politehnica of Bucharest 2013;75:121-128.
[24] Robert M. Jones 'Mechanics of Composite Materials, Second Edition' Book, Taylor and Francis, 1999.
[25] Valery V. Vasiliev and Evgeny V. Morozov 'Mechanics and Analysis of Composite Materials' Book, Elsevier Science Ltd, 2001.
[26] By Angelo R, Maligno L. Finite element investigations on the microstructure of composite materials. PhD thesis The University of Nottingham, UK, 2007.
[27] Isaac MD, Ishai O. Engineering mechanics of composite materials, (Second Edition), Oxford University Press ISBN 019515097X, New-York; USA, 2005.
[28] Shaofan L, Gang W. Introduction to micromechanics and nano-mechanics, World Scientific Pub., ISBN 978-981-281-413-2; 2008.
[29] Kollar LP, Springer GS. Mechanics of composite structures. Cambridge University Press, UK, 2003.
[30] Laszlo P. Kollar and George S. Springer 'Mechanics of Composite Structures' Book, Cambridge University Press, 2003.
[31] Satish KG, Siddeswarappa B, Mohamed KK. Characterization of in-plane mechanical properties of laminated hybrid composites. J Miner Mater Character Eng 2010;9(2):105-114.
[32] Gao XL, Li K, and Mall S. A mechanics-of-materials model for predicting Young's modulus of damaged woven fabric composites, involving three damage modes, Int J Solids Struct 2003;40:981–999.
[33] Valery V. Vasiliev and Evgeny V. Morozov 'Advanced Mechanics of Composite Materials, Second Edition' Book, Elsevier Ltd, 2007.
[34] Farooq U, Myler P. Explicit Dynamic Simulation of Flat Nose Low Velocity Impact of Relatively Thick Composite Panels Using Built-In Failure Criteria. International Journal of Scientific Engineering and Science (IJSES) 2021;5(6):35-51.
[35] Farooq U, Myler P. Stress base modelling and computer simulation of drop-weight impact response of composite panels with domain partitioning and adaptive meshing techniques. International Journal of Recent Research and Applied Studies (IJRRAS) 2021;8(4),38-58.

Corresponding author: [1*]Umar Farooq
Emails: adalzai3@yahoo.co.uk and U.Farooq@bolton.ac.uk
Reader in Department of Engineering and Design
University of Bolton, Bolton BL3 5AB UK
Phone and fax: 0044-1204 903011